NUMERICAL AND EXPERIMENTAL STUDY ON THE DETAILED MECHANISM OF H_2–AIR FLAME JET IGNITION

Bitoh, H., Seutake, M., Asahara, M., Yamada, E., Hayashi, A.K.
Dept. of Mechanical Engineering, Aoyama Gakuin University,
5-10-1, Fuchinobe, Chuou-ku, Sagamihara city, Kanagawa, Japan

ABSTRACT

Jet ignition was recognized in the 1970s, and has since been applied to automobile engines such as the Honda CVCC. In the 1990s, jet ignition was observed in explosions and was seen as a problem that may relate to jet ignition. Our group presented jet ignition experimentally and numerically in 1999, and later using LIF measurements with the same experimental vessel as used in 1999. However, the detailed mechanism of jet ignition was not clarified at that time. The target of this study is to clarify how jet ignition happens and to understand the detailed mechanism of flame jet ignition.

1. INTRODUCTION

A lot of attention has been paid to hydrogen as a next-generation fuel. Hydrogen produces only water from its combustion, unlike hydrocarbons. However, its burning rate is so fast that it may easily cause explosions. Two years ago, we had the Fukushima Daiichi Nuclear Power Plant accident after the large earthquake, which might have been triggered by the jet ignition of hydrogen. The first application of jet ignition was probably by Gussak in 1976 (1) and 1983 (2) , who developed the avalanche activated combustion (LAG) jet ignition engine. With this method, we can burn a reasonably lean mixture of fuel that cannot be ignited by a conventional spark igniter. Oppenheim studied and developed a fuel jet igniter to apply to a real engine in the 1980s (3) and 1990s (4) . He used a plasma jet igniter (PJI) and a flame jet igniter (FJI) and compared them for their energy efficiency. Since the FJI uses a conventional sparkplug, Oppenheim used it for an automobile engine igniter. One good example of an FJI igniter applied to an engine can be found in the work done by Hensinger et al. (5).

Suetake et al. (6) studied the fundamentals of jet ignition experimentally and numerically in 1999. They used a chamber with two rooms divided by a wall with a hole at its center. The map of the ignition in the receiver chamber with a hydrogen/air mixture is shown in Fig. 1 by equivalence ratio as a function of orifice size. They mapped three types of ignition: jet ignition, transient ignition, and auto ignition. Auto ignition in their case implies that the ignition occurred in the receiver chamber just before the flame went through the hole in the divided wall. The experimental chamber configuration is shown in Fig. 2. Later, Asami et al. (7) measured OH profiles of jet ignition using a laser-induced fluorescence (LIF) measurement system to see the development and propagation mechanism of jet ignition. At almost same time, Jordan et al. studied jet ignition in a similarly configured combustion chamber, but they did not observe so-called auto-ignition.

The present study will show the detailed mechanism of flame jet ignition numerically using a detailed chemical reaction mechanism of hydrogen together with some of Suetake's experimental results.

2. EXPERIMENTAL RESULTS

The schematic diagram of the experimental setup is shown in Fig. 2. The combustion chamber consists of two rooms of different sizes that are partitioned by a wall with an orifice. The driver chamber (DC) has a size of 150 mm × 160 mm with a sparkplug at its bottom, and the receiver chamber (RC) has a size of 30 mm × 30 mm × 80 mm. The orifice diameters are 5, 8, 10, and 12 mm. The combustion chamber has two quartz glass optical windows for a Schlieren visualization system. A diagram of the Schlieren visualization system is shown in Fig. 4. Pressure is measured by two pressure transducers at the centers of sidewalls, one each for the driver chamber and the receiver chamber. The pressure measurement system is also shown in Fig. 4. The signal output from the pressure element passes through the amplifier and is fed to the oscilloscope as input. For processing data from pressure element by the PC, the data is transferred to the PC thorough a general-purpose interface bus (GPIB) board, which is connected, to an oscilloscope and converts the data into a file using LabVIEW ver4.0. A commercial automobile sparkplug is used to ignite the gas at the bottom

center of DC. The flame is ignited by the sparkplug to propagate in the DC and pass through the orifice to be reignited in the RC. The experiments are carried out using premixed hydrogen/air mixture at the equivalence ratios of 0.235, 0.250, 0.257, 0.264, 0.272, 0.279, 0.294, 0.309, 0.325, 0.340, and 0.356. The initial condition is held at atmospheric pressure and room temperature, which is kept consistent for the different initial concentrations and orifice diameters. A typical Schlieren system is set to visualize the jet ignition phenomena using a Kodak high-speed video camera for recording.

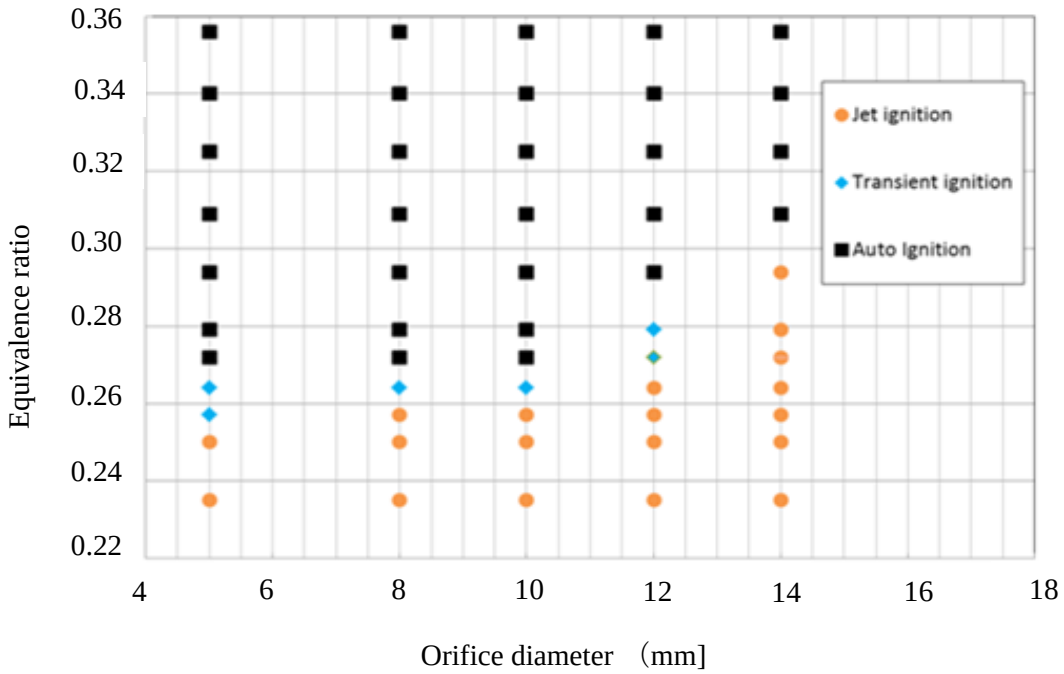

Figure 1. Combustion mode of jet ignition.

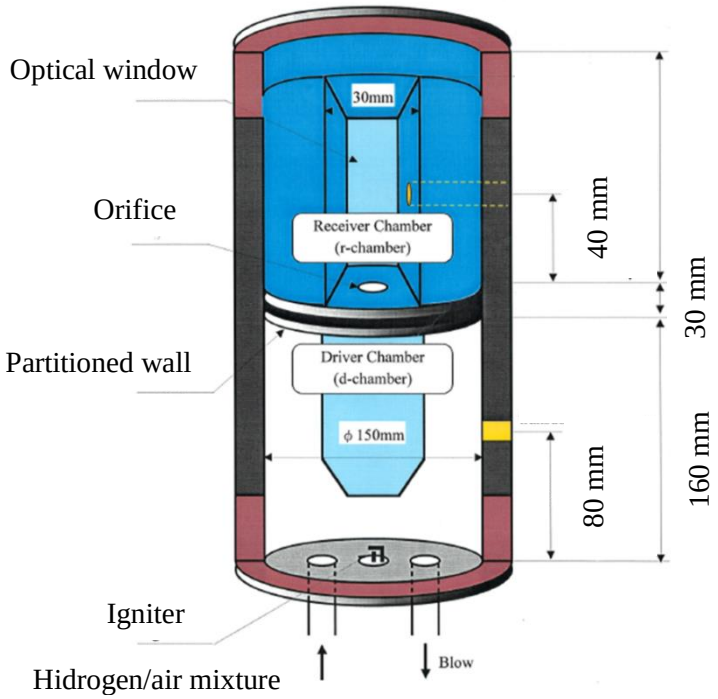

Figure 2. Combustion chamber.

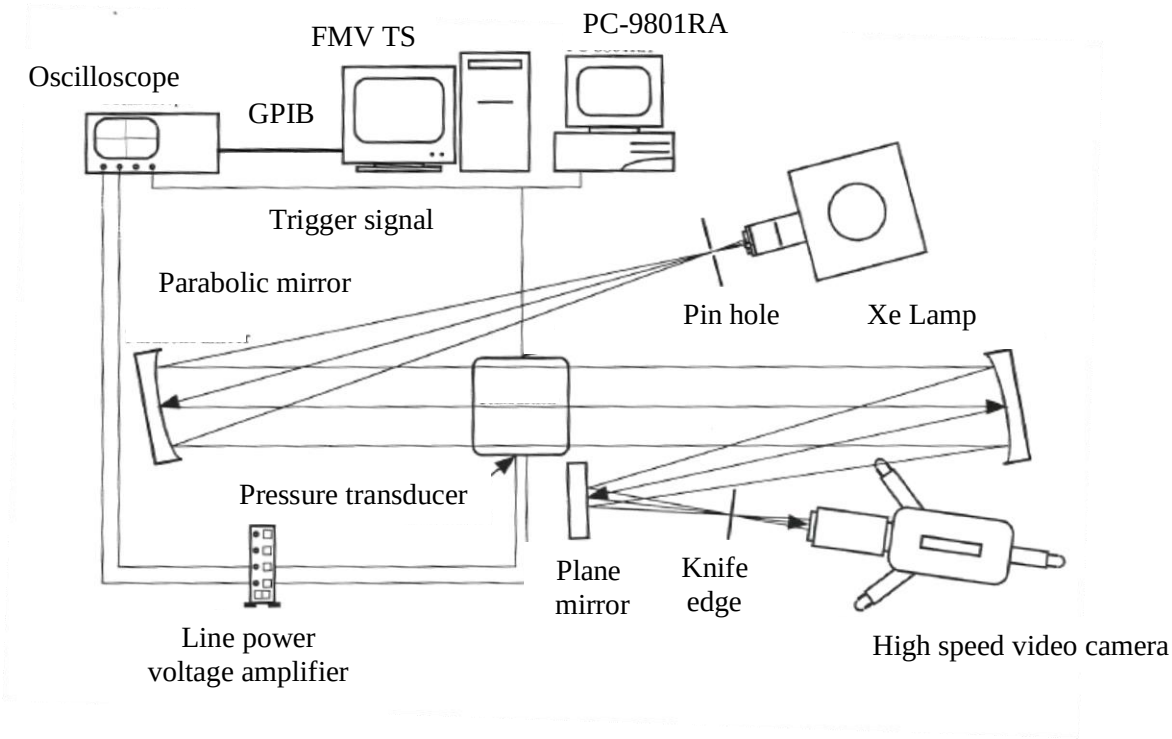

Figure 3. Diagram of measurement system.

3. FORMULATION AND NUMERICAL METHODS

Flame jet ignition is simulated 2-dimensionally using the Navier–Stokes equations with a hydrogen–air full chemical reaction model consisting of 9 species and 19 reaction mechanisms (8). The Navier–Stokes equations are integrated by the Harten–Yee, non-MUSCL modified-flux type TVD-upwind scheme for the convection terms, the Crank–Nicholson semi-implicit scheme for the species production terms, and the second-order central difference method for the viscous terms. The generalized Roe's average is applied for the averaged state on cell boundaries to evaluate numerical flux in the convective terms. A Strange-type fractional-step method is used for time integration to keep the integration at the second order. The equation of continuity and the momentum and energy equations are:

$$\frac{\partial Q}{\partial t}+\frac{\partial}{\partial x}(F_1+G_1)+\frac{\partial}{\partial y}(F_2+G_2)=\dot{S}, \qquad (1)$$

$$Q=\begin{bmatrix} e \\ \rho \\ \rho u \\ \rho v \\ \rho_i \end{bmatrix}, F_1=\begin{bmatrix} (e+p)u \\ \rho u \\ \rho u^2+p \\ \rho v u \\ \rho_i u \end{bmatrix}, F_2=\begin{bmatrix} (e+p)u \\ \rho v \\ puv \\ \rho v^2+p \\ \rho_i v \end{bmatrix}, G_1=\begin{bmatrix} \dot{q}_x-u\tau_{xx}-v\tau_{xy} \\ 0 \\ -\tau_{xx} \\ -\tau_{xy} \\ \rho_i u \end{bmatrix}, G_2=\begin{bmatrix} \dot{q}_y-u\tau_{yx}-v\tau_{yy} \\ 0 \\ -\tau_{yx} \\ -\tau_{yy} \\ \rho_i v \end{bmatrix},$$

$$S = \begin{bmatrix} e \\ \rho \\ \rho u \\ \rho v \\ \dot{\omega}_i \end{bmatrix},$$

$$\tau_{xx} = 2\mu \frac{\partial u}{\partial x} - \frac{2}{3}\mu \emptyset,$$

$$\tau_{yy} = 2\mu \frac{\partial v}{\partial x} - \frac{2}{3}\mu \emptyset,$$

$$\tau_{xy} = \tau_{yx} = \mu \left(\frac{\partial u}{\partial y} + \frac{\partial v}{\partial x} \right),$$

where ρ is the density, u and v are the velocities in the x and y directions, respectively, e is the total energy, i is the number of the chemical species (i = 1, 2, ..., N), N is the total number of species, ρ_i is the density of the i^{th} species, p is the pressure, and $\dot{\omega}_i$ is the production rate of the i^{th} species by the chemical reaction. Figure 4 shows the computational region in this study, and Table 1 shows the initial conditions. The computational region is scaled down to 1/10 of the experimental region. The computational grid square is 50 μm. The ignition region is a circle with a diameter of 0.2 mm, and the center of the ignition area is located 1.5 mm from the bottom center.

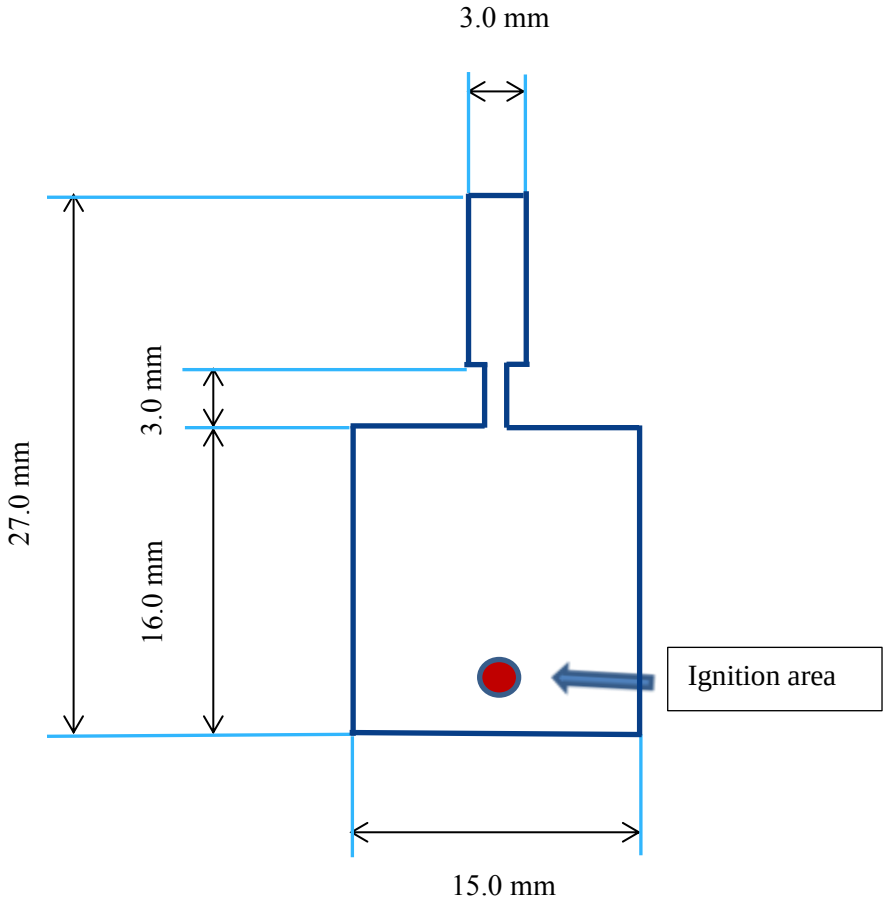

Figure 4. Computational region and Ignition location.

Table.1 Initial conditions

Initial pressure [MPa]	0.10
Initial temperature [K]	293
Equivalent ratio	0.340

4. EXPERIMENTAL FINDINGS

4.1 Jet ignition

The Schlieren photos of jet ignition are shown in Fig. 5. The initial conditions are an equivalence ratio of 0.250 and an orifice diameter of 10 mm. From the photos, the flame came out through the orifice at 311.7 ms (the first photo of the left side) and its head moved to 17.8 mm from the bottom in the RC. At 311.7 ms, compression waves were propagating towards the top of the RC and bouncing back, probably many times. At 312.0 ms the ignition started at the top head of the flame jet, and at 312.5 ms, the flame structure expanded in the radial direction with an umbrella shape. Jet ignition occurred sometime between 312.0 and 312.5 ms, where many activated species such as O, H, and OH provide an ignition source. Since there is drag between the jet and the stationary air, the flame jet propagation speed is reduced.

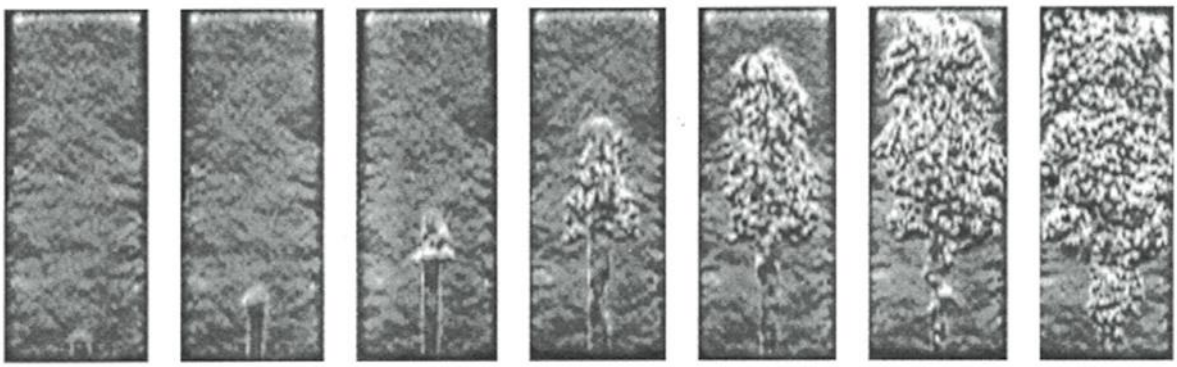

Figure 5. Schlieren photograph (Equivalent ratio 0.250, orifice diameter 10 mm).

The pressure history at the center of the RC wall and the corresponding Schlieren photos for the case of an equivalence ratio of 0.250 and an orifice diameter of 10 mm are shown in Fig. 6. The Schlieren photos correspond to the region that is marked in the plot of pressure history by the colored mesh around 190 ms. This indicates typical jet ignition. Although the phenomena seen in the Schlieren photos show a complicated compression wave interaction, the pressure record does not show such complicated phenomena, but rather it shows a gradual increase of pressure compared with other region of pressure history. The pressure peak can be seen at around 205 ms. It is clarified that the pressure in the RC does not rise rapidly and immediately with the flame entering the RC.

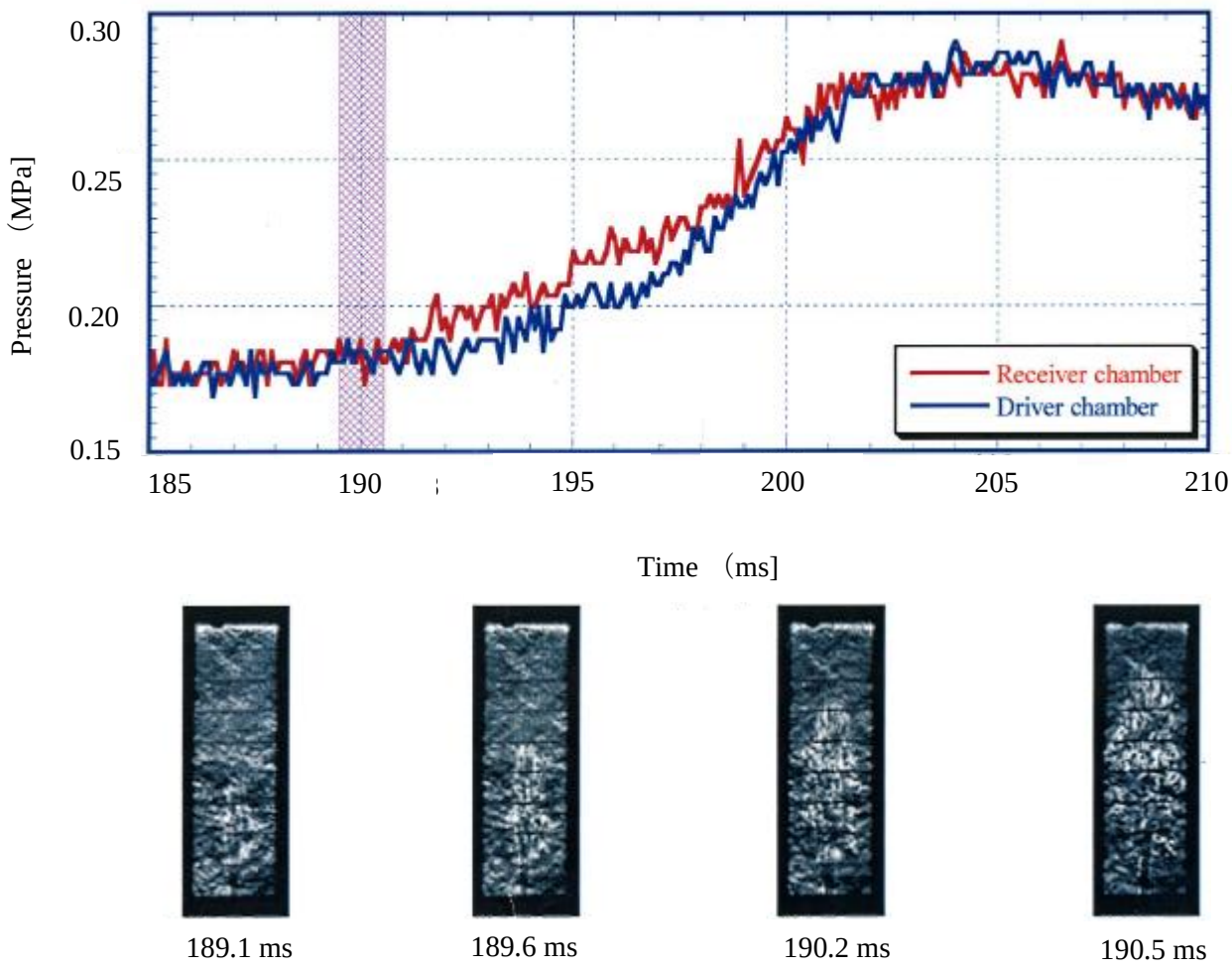

Figure 6. Pressure history (top) and Schlieren photographs (bottom) (Equivalent ratio 0.250, orifice diameter 10 mm).

4.2 Auto ignition

Images of auto ignition in the receiver chamber are shown in Fig. 7 where the mixture condition is at an equivalence ratio of 0.356 with an orifice diameter of 10 mm. From the left photo to the right end photo we cannot see the flame jet coming out of the orifice. However, before the flame jet goes through the orifice, we can see that ignition starts near the right corner of the top wall in RC at 51.4 ms. This phenomenon occurs under certain conditions such as higher equivalence ratios, which are shown in the jet ignition map of Fig. 1. The flame does not have a clear shape, and at 52.0 ms, it propagates rapidly downward.

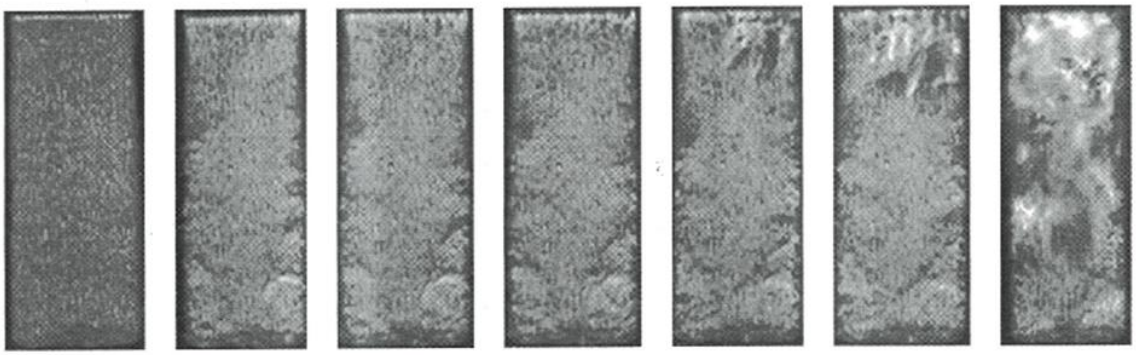

Figure 7. Schlieren photograph (Equivalent ratio 0.356, orifice diameter 10 mm).

The pressure history at the center of the RC wall and the corresponding Schlieren photos for the case of an equivalence ratio of 0.356 and an orifice diameter of 10 mm are shown in Fig. 8. The Schlieren photos correspond to the region, which is marked in the figure of pressure history by the colored mesh around 73 ms. This case is a typical auto ignition. The photos were taken at the frame rate of 40,500 fps. Auto ignition is observed at the left corner at 72.98 ms, and the flame propagates downward rapidly at an estimated velocity of 42 m/s. The pressure in the RC increases sharply after 74 ms due to ignition. It seems that the ignition does was not caused by pressure but probably by a temperature increase due to adiabatic compression.

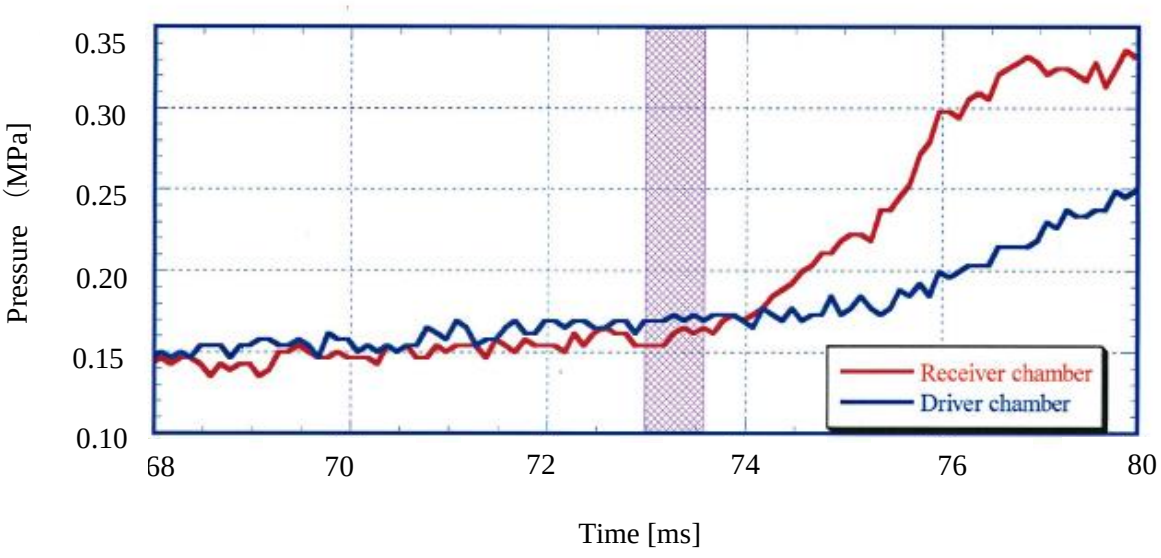

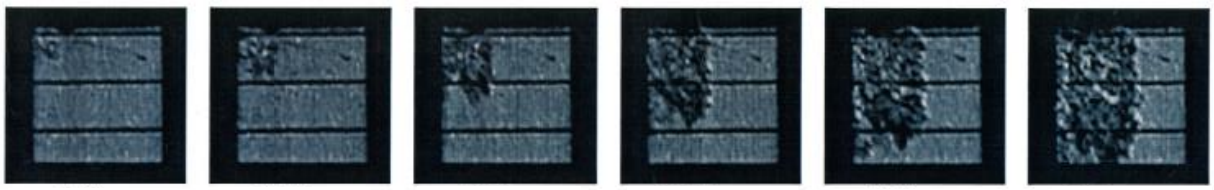

Figure 8. Pressure history (top) and Schlieren photographs (bottom) (Equivalent ratio 0.356, orifice diameter 10 mm).

5. RELATIONSHIP OF TIME TO REACH THE FIRST PEAK PRESSURE

The time to reach the first peak pressure (TRFPP) is plotted as a function of equivalence ratio and orifice diameter in Fig. 9. When the equivalence ratio is high, the time to reach ignition is short, which means that the higher equivalence ratio implies a higher energy to reach auto-ignition. The time difference between the longest time and the shortest time for ignition is about 170 ms. This difference comes from the flame propagation velocity in the RC. The blue and red hatched regions correspond to jet ignition and auto ignition, respectively. TRFPP in the case of jet ignition has a 50-ms at maximum difference among orifice diameters: a smaller diameter gives a shorter TRFPP, and a larger diameter provides a longer TRFPP. The jet ignition case heavily relies on flame propagation in the RC. The flame propagation velocity depends on the orifice size.

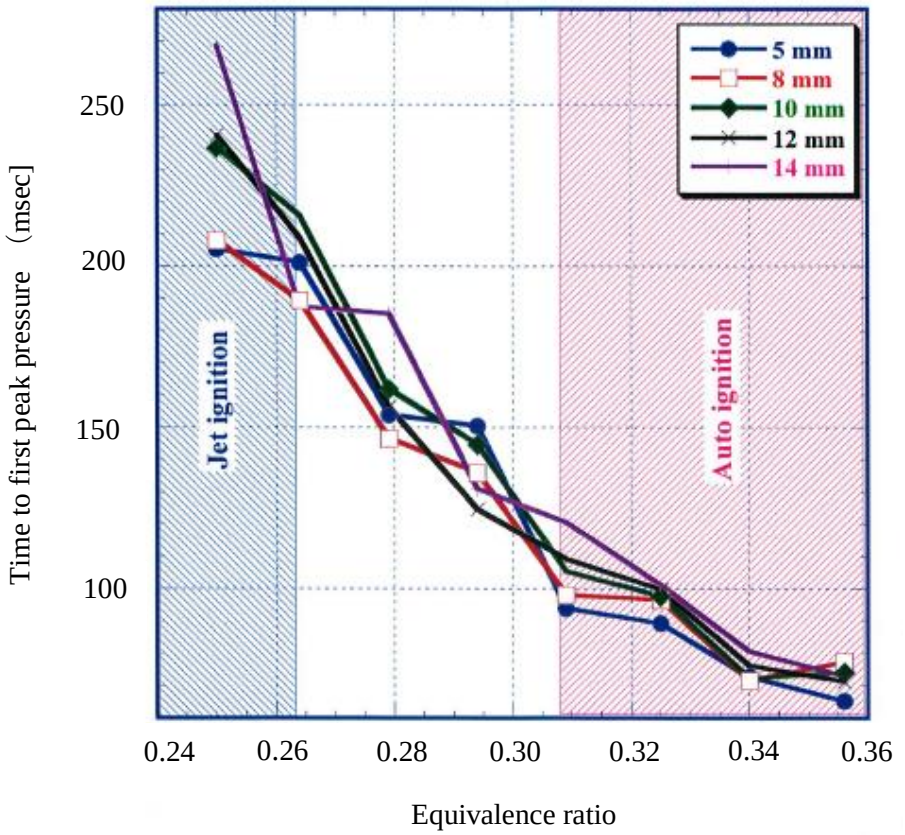

Figure 9. Time to reach first peak pressure in the receiver chamber.

6. NUMERICAL RESULTS

Figure 10 shows the temperature distributions in the DC and RC at 1.6-μs intervals from the time the flame enters the RC. It shows that the flame forms a mushroom shape when it enters the RC. The tip of the mushroom-shaped flame forms a vortex, and it propagates in the lateral direction. The flame extends rapidly downward because the jet flow has high speed and high pressure at the orifice. A mushroom-shaped flame is formed in such a case depending on conditions. Jordan et al. (9) said that the vortex formed by such a mushroom-shaped flame with mixing of the burned gas and unburned gas causes the jet ignition. Suetake said that one of the main unknown phenomena in auto ignition is the compression wave interface at the corner in the RC. Suetake et al. proposed that there is a possibility that the compression wave interaction with other compression waves at a corner while approaching at

the same angle results in auto ignition. Figure 11 shows the pressure history in the present calculation. The concentration of compression waves at the corner of the RC has been captured, while that in the RC cannot be captured. Since the calculations are performed in a computational domain of 1/10 scale, flame reaches the RC earlier than in the experiment. The calculation does not catch enough reciprocating motion of the compression wave.

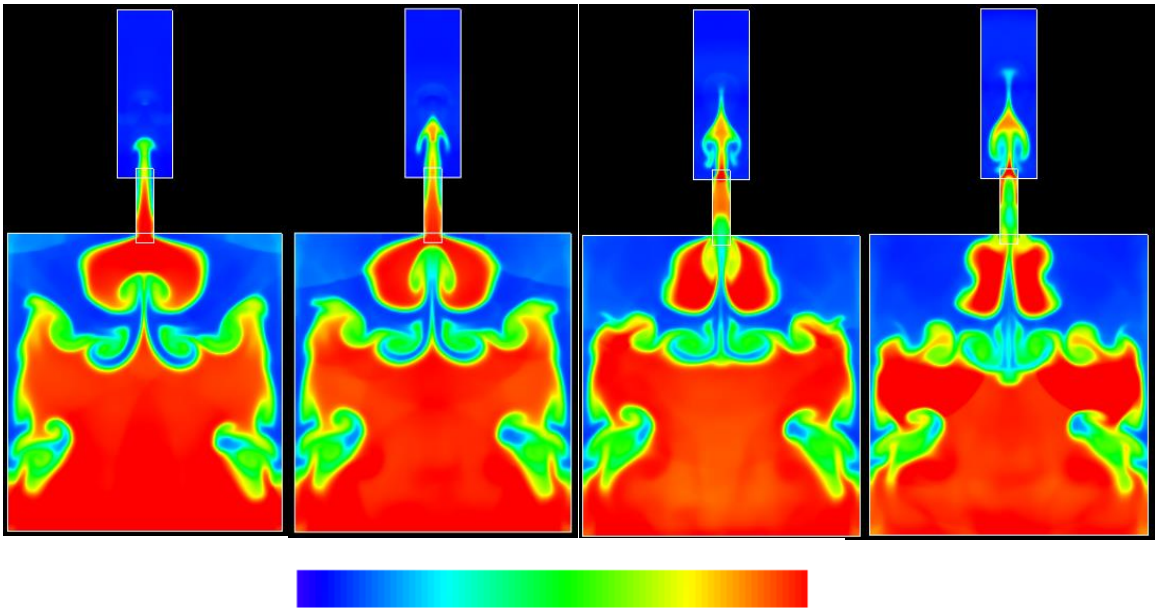

293 K 2300 K

Figure 10. Time history of temperature distribution.

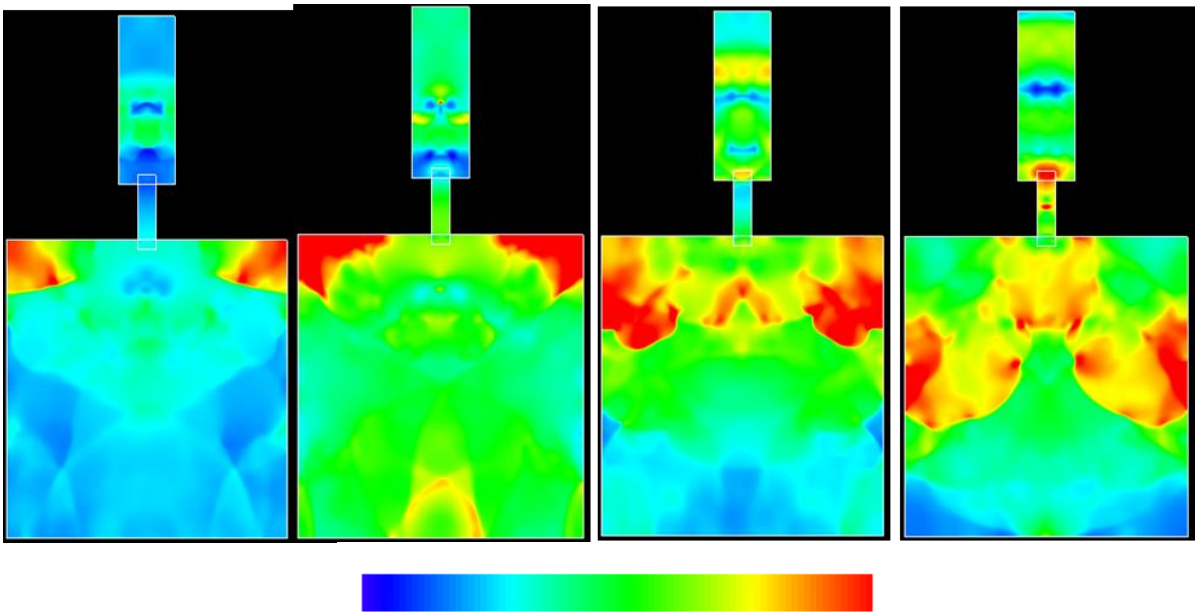

0.08 MPa 0.3 MPa

Figure 11. Time history of pressure distribution.

7. CONCLUSIONS

- A mushroom-shaped flame enters the RC to form a vortex in the same mechanism as in the experiment.
- The vortex formed by the mushroom-shaped flame is a mixture of burned and unburned gas, which promotes combustion.
- Jet ignition and auto ignition were observed depending on the initial conditions.
- Orifice diameter and hydrogen concentration play important roles to determine whether jet ignition or auto ignition occurs.

REFERENCES

1. Gussak L.A., High Chemical Activity of Incomplete Combustion Products and a Method of Pre-chamber Torch Ignition for Avalanche of Combustion in Internal Combustion Engines. SAE Transactions: 1976.
2. Gussak L.A., The Role of Chemical Activity and Turbulence Intensity in Pre-chamber Torch Organization of Combustion of a Stationary Flow of a Fuel–Air Mixture.
3. Oppenheim A.K., Quest for Controlled Combustion Engines. SAE Transactions, The Jornal of Engines: 1998.
4. Oppenheim, A.K., Beltramo, J., Faris, D.W., Maxson, J.A., Hom, K., Stewart, H.E. Combustion by Pulsed Jet Plumes – Key to Controlled Combustion Engines. SAE SAE Transactions, The Journal of Engine: 1989.
5. Hensinger, D.M., Maxson, J.A., Hom, K., Oppenheim, A.K. Jet Plume Injection and Combustion. SAE 920414, SAE Transactions: 1992.
6. Suetake, M., Uchida, N., Hayashi, A.K. Experimental and Numerical Analysis of Jet Ignition. Proceedings of 17th ICDERS: 1999.
7. Asami, K., Sakamoto, K., Hayashi, A.K., Measurements of Jet Ignition in Premixed Hydrogen/Air Mixture. Proc. of 7th JSME General Meeting: 2001.
8. Petersen, E.L., Hanson, R.K., Reduced Kinetics Mechanism for Ram Accelerator Combustion. Journal of Propulsion and Power: 1999.
9. Jordan, M., Eder, A., Edlinger, B., Mayinger, F., Turbulent Quenching and Acceleration of Flames by Highly Blocking Obstacles. FISA Symposium: 1999.
10. Mittint, D.N.R., Dabora, E.K., Flame Jet Ignition of Lean Fuel–Air Mixtures. Dynamics of Reactive Systems, vol 105.
11. Gaathaug, A.V., Bjeketvedt, D., Vaagsaether, K., Experiments with Flame Propagation in a Channel with a Single Obstacle and Premixed Stoichiometric H_2-Air. Combustion Science and Technology vol 182, 2010, pp 1693–1706.
12. Eder, A., Gerlach, C., Mayinger, F., Experimental Observation of Fast Deflagration and Transition to Detonations in Hydrogen–Air Mixtures.